



Multi-dimensional phase portraits of stochastic fractional derivatives for nonlinear dynamical systems with solitary wave formation

Ali R. Ansari¹ · Adil Jhangeer^{2,6} · Mudassar Imran³ · A. S. A. Alsubaie⁴ · Mustafa Inc⁵

Received: 18 October 2023 / Accepted: 11 January 2024 / Published online: 29 March 2024
© The Author(s) 2024

Abstract

This manuscript delves into the examination of the stochastic fractional derivative of Drinfel'd-Sokolov-Wilson equation, a mathematical model applicable in the fields of electromagnetism and fluid mechanics. In our study, the proposed equation is through examined through various viewpoints, encompassing soliton dynamics, bifurcation analysis, chaotic behaviors, and sensitivity analysis. A few dark and bright shaped soliton solutions, including the unperturbed term, are also examined, and the various 2D and 3D solitonic structures are computed using the Tanh-method. It is found that a saddle point bifurcation causes the transition from periodic behavior to quasi-periodic behavior in a sensitive area. Further analysis reveals favorable conditions for the multidimensional bifurcation of dynamic behavioral solutions. Different types of wave solutions are identified in certain solutions by entering numerous values for the parameters, demonstrating the effectiveness and precision of Tanh-methods. A planar dynamical system is then created using the Galilean transformation, with the actual model serving as a starting point. It is observed that a few physical criteria in the discussed equation exhibit more multi-stable properties, as many multi-stability structures are employed by some individuals. Moreover, sensitivity behavior is employed to examine perturbed dynamical systems across diverse initial conditions. The techniques and findings presented in this paper can be extended to investigate a broader spectrum of nonlinear wave phenomena.

Keywords Stochastic fractional derivatives · Soliton solutions · Nonlinear dynamical system · Multidimensional bifurcation · Multi-stability

1 Introduction

The majority of dynamical phenomena in nature are intrinsically nonlinear and are characterized by nonlinear partial differential equations (NLPDEs), which can be either continuous or discontinuous. Knowing their accurate or reasonable results is critical for comprehending most natural events. They are generally divided into two types: integrable and non integrable structures. While integrable problems can be easily analyzed analytically using well-known approaches such as the Inverse Scattering Transform (Ablowitz et al.

1974), the Hirota method (Hirota 2004), and the Darboux transformation method (Matiyev and Salle 1991), non integrable systems can only be examined in general situations through numerical simulations (Hoffman and Frankel 2018; Imkeller and Monahan 2002). The NLPDEs have traveling wave solutions, which have become a fundamental aspect of research in nonlinear wave dynamics and have been explored in various disciplines such as optical fibers, plasma, fluid dynamics, elastic media, and so on. Numerous strategies for obtaining various soliton solutions to these NLPDEs have been discovered in the literature. Among these are the square operator approach (Wang et al. 2022), the unified technique (Vivas-Cortez et al. 2023), Hirota's bilinear approach (Geng et al. 2023, Geng et al. 2023), the neural network approach (Xu et al. 2023), the extended tanh-function approach (Zaman et al. 2023a, b), and many others (Arefin et al. 2022; Zaman et al. 2023). They have enhanced the dynamic approach by employing various methods, such as the generalized Kudryashov method (Akbar et al. 2022), the sinh-Gordon equation expansion method (Akbar et al. 2021), the (G'/G) -expansion (Islam et al. 2022), the tanh technique (Almusawa et al. 2022), the rational $(1/\Phi')$ -expansion approach (Islam et al. 2022).

Considerable investigation has previously been carried out to explore the dynamics of solitons, utilizing various nonlinear models, including Schrödinger model (Bo et al. 2023; Wen et al. 2023), Fractional foam drainage model (Yokuş et al. 2022), Bogoyavlenskii equation (Islam et al. 2023), shallow water equation (Akbar et al. 2023), and Modified equal-width equation (Khatun et al. 2022). One or more stochastic processes are used as terms in a stochastic differential equation (SDE), and another stochastic process is employed as the solution. SDEs are utilized to replicate a wide variety of phenomena, including stock prices and physically based models susceptible to thermal changes. Consequently, SDEs have become crucial for simulating phenomena in various fields such as biology, chemistry, physics, marine biology, and fluid dynamics (Prévôt and Röckner 2007).

Over the past decade, physicians have been passionately investigating various types of nonlinear solitonic systems in plasmas, including single waves, shock waves, and surface waves. Due to the presence of different volumes of dust grains in plasma, different types of wavelengths have been observed, such as acoustic mode (Akinyemi et al. 2021), dust Bernstein-Green-Kruskal mode (El-Taibany and Sabry 2005), dust acoustic mode (Anderson and Ulness 2015), and dust-up mode (low-wave mode) (Yang et al. 2012). In recent years, according to a research study, numerous literature works have focused on exploring the behavior of new waves (Bains et al. 2010), the imbalance of quantum beams (Ahmed et al. 2018), quantum modifications to the Zakharov equations, and quantum ion-acoustic waves (Gupta et al. 2015). Recently, the separation of ion-acoustic dust waves into magnetic dust plasma using the q -nonextensive velocity circulation, based on the bifurcation concept of balanced dynamical structures, has been investigated in several articles (Jansen et al. 2009). These articles have examined the differentiation of nonlinear waves in plasma physics (Jahan et al. 2019). Therefore, the main objective of our current research is to discover new systematic solutions for acoustic dust waves and nonlinear LWE (Long-Wave Equation), which are clearly defined by the size and dimensions of the 2D and 3D structures (Ghosh et al. 2012; Baluku and Hellberg 2008).

A fascinating area of study in recent times has been the application of bifurcation analysis to the study of differential equations (Liu et al. 2022; Talafha et al. 2023). Several authors have conducted research on the concepts of dynamic system bifurcation within both disturbed and unperturbed frameworks (Saha 2017). Samina et al. (2022) derived the bifurcation behavior, chaotic dynamics, and multistability analysis of the $(2+1)$ -dimensional elliptic nonlinear Schrödinger equation with external perturbation, utilizing bifurcation and

chaos theories. Sprott (2011) investigated the prevalence of chaotic systems and identified them. The focus of the present study is to explore the temporal, quasi-periodic, sensitivity, and solitonic behavior of dust acoustic waves in three distinct plasma volumes with inertial ion-negative components. By considering the external influences of disturbances, we aim to understand the quasi-periodic behavior and the sensitivity of the disturbance scheme in non-magnetic plasma based on our expertise.

The mathematical modeling of exact processes that require accurate damping modeling is accomplished using fractional derivative approaches. Fractional derivatives offer advantages such as adaptability and non-locality. Unlike ordinary derivatives, these derivatives possess fractional order, which grants them greater flexibility in approximating actual information. Additionally, they incorporate non-locality, a feature lacking in ordinary derivatives. Fractional derivatives find application in various significant phenomena, including anomalous diffusion, electro-chemistry, acoustics, computational imaging, and magnetic fields. Fractional models tend to provide higher accuracy compared to integer models. However, solving fractional derivative stochastic differential equations (SDEs) is generally more challenging than solving conventional ones. In light of this, we have focused on examining the SFDSW equations as presented in Al-Askar et al. (2022).

$$dw + [\beta y D_{\eta}^{\phi} y] d\zeta = \alpha w d\mu, \quad (1)$$

$$dy + [m_1 D_{\eta\eta}^{\phi} y + m_2 w D_{\eta}^{\phi} y + m_3 y D_{\eta}^{\phi} w] d\zeta = \alpha y d\mu. \quad (2)$$

Here $w = w(\eta, \zeta)$, $y = y(\eta, \zeta)$. β , m_j , $j = 1, 2, 3$ are non-zero parameters. The conformable derivative (CD) is denoted as D^{ϕ} , $0 < \phi \leq 1$. The function $\mu = \mu(\zeta)$ corresponds to a standard Brownian motion (SBM), and α represents the noise strength.

Equation (1) and (2) are an expanded version of the standard DSW. When $\phi = 1$, and $\alpha = 0$, then the above system transforms into the standard DSW equation, initially proposed by Drinfeld and Sokolov (1981); Sokolov (1984), and later refined by Wilson (1982). Furthermore, this model finds applications in plasma physics, various applied sciences, fluid and population dynamics, and electromagnetism. Given the significance of DSW model, numerous scholars have developed diverse methodologies to investigate exact solutions of the system, including Hirota's bilinear (Alsallami et al. 2023), Jacobi elliptical function (Sahoo and Ray 2017), (G'/G) -Expansion method (Al-Askar et al. 2022), complete discrimination for polynomial (Zhang and Han 2023), He's variational approach (Wang and Wang 2023), truncated Painlevé (Ren et al. 2016), and mapping approach (Al-Askar et al. 2022).

This investigation will primarily focus on achieving its objectives from three distinct perspectives. Firstly, it aims to establish various soliton profiles through the application of a tanh method. Secondly, a pivotal aspect involves conducting a parameter-based analysis of the system under scrutiny, incorporating bifurcation and chaos theories. The detailed explanation of the bifurcation of the unperturbed system is illustrated through phase portraits. Additionally, the chaotic analysis of the perturbed system is determined and demonstrated using various tools, including time series and phase portraits. Furthermore, the study delves into the sensitivity and multistability of the examined system. The authors emphasize the novelty of this study, asserting that it presents an interesting perspective not previously explored for the considered system.

The outline of the paper is as follows: Sections (2) and (3) provide preliminary information and present the mathematical model. The solution analysis for the proposed approach

is discussed in Section (4). Section (5) focuses on the physical interpretation of the evaluated model. The bifurcation theory of the model under study is examined in Section (6). Section (7) explores the periodic and quasiperiodic properties of the model. The sensitivity analysis of the model is conducted in Section (8). Section (9) investigates the multistability of the model. The conclusion is presented in the final section of the paper.

2 Preliminaries

The suitable derivative and conventional Brown’s law are now being examined in terms of their characteristics and descriptions. The following is the definition of a suitable derivative:

Definition 2.1 The function’s conformable derivative (Al-Askar et al. 2022)

$$r = r(\eta) : [0, \infty) \rightarrow \mathbb{R}$$

for the independent variable η of the order ϕ , it is given as:

$$D_\eta^\phi r(\eta) = \lim_{\beta \rightarrow \infty} \frac{r(\eta + \beta \eta^{1-\beta}) - r(\eta)}{\beta}, \quad \eta > 0, \quad \phi \in (0; 1].$$

2.1 Properties

If $g = g(\eta)$ and $r = r(\eta)$ are ϕ -differentiable for all positive η ,

- $D_\eta^\phi(T_1g + T_2r) = T_1D_\eta^\phi(g) + T_2D_\eta^\phi(r), \quad \forall T_1, T_2 \in \mathbb{R},$
- $D_\eta^\phi(z^z) = z^{z-\phi}, \quad z \in \mathbb{R},$
- $D_\eta^\phi(\lambda) = 0, \quad \forall r(\eta) = \lambda \in \mathbb{R},$
- $D_\eta^\phi(gr) = gD_\eta^\phi r + rD_\eta^\phi g,$
- $D_\eta^\phi\left(\frac{r}{g}\right) = \left(\frac{gD_\eta^\phi(r) - rD_\eta^\phi(g)}{g^2}\right),$
- $D_\eta^\phi(r)(\eta) = \eta^{(1-\phi)} \frac{dr}{d\eta},$
- $D_\eta^\phi(r \circ g)(\eta) = \eta^{(1-\phi)} g'(\eta) r'(g(\eta)).$

Lemma (Calin 2015) $E(e^{\omega\mu(\zeta)}) = e^{\frac{1}{2}\omega^2\zeta}, \quad \omega \geq 0.$

3 Mathematical model

3.1 Description of method

Assume that NLPDE with unknown variables (η, ζ) are given by,

$$H(Y, Y_\eta, Y_\zeta, Y_{\eta\eta}, Y_{\zeta\zeta}, \dots) = 0, \tag{3}$$

where H is the polynomial including the unknown function $Y(\eta, \zeta)$. For obtaining the traveling wave patterns, the following transformation is used:

$$w(\eta, \zeta) = W(\xi)e^{(\alpha\mu(\zeta) - \frac{1}{2}\alpha^2\zeta)}, \quad y(\eta, \zeta) = Y(\xi)e^{(\alpha\mu(\zeta) - \frac{1}{2}\alpha^2\zeta)} \quad \text{where } \xi = \frac{1}{\lambda}\eta + \kappa\zeta, \quad (4)$$

here W and Y are real deterministic functions. By plugging Eq. (4) in (3) to attain the nonlinear ODE as following,

$$G(Y, Y', Y'' \dots) = 0, \quad (5)$$

consider the result of Eq. (5) has a model,

$$Y(\xi) = \sum_{i=0}^n l_i U^i(\xi), \quad (6)$$

where

$$U(\xi) = \tanh(\xi), \quad (7)$$

then $Y'(\xi)$ and $Y''(\xi)$ can be written as:

$$\frac{dY}{d\xi} = 7(1 - U^2) \frac{dY}{dU}, \quad (8)$$

$$\frac{d^2Y}{d\xi^2} = (1 - U^2)(-2U \frac{dY}{dU} + (1 - U^2) \frac{d^2Y}{dU^2}). \quad (9)$$

4 Solution analysis for the SFDSW model

Plugging Eq. (4) in Eqs. (1) and (2), we attain the ordinary differential equation which perhaps reported as:

$$\begin{aligned} dw &= [\kappa W' d\zeta + \alpha W d\mu] e^{(\alpha\mu(\zeta) - \frac{1}{2}\alpha^2\zeta)}, \\ dy &= [\kappa Y' d\zeta + \alpha Y d\mu] e^{(\alpha\mu(\zeta) - \frac{1}{2}\alpha^2\zeta)}, \\ D_{\eta}^{\lambda} w &= W' e^{(\alpha\mu(\zeta) - \frac{1}{2}\alpha^2\zeta)}, \\ D_{\eta}^{\lambda} y &= Y' e^{(\alpha\mu(\zeta) - \frac{1}{2}\alpha^2\zeta)}, \\ D_{\eta\eta}^{\lambda} w &= Y''' e^{(\alpha\mu(\zeta) - \frac{1}{2}\alpha^2\zeta)}. \end{aligned} \quad (10)$$

Plugging Eq. (10) in Eqs. (1) and (2), we get:

$$\kappa W' + \beta Y Y' e^{(\alpha\mu(\zeta) - \frac{1}{2}\alpha^2\zeta)} = 0, \quad (11)$$

$$\kappa Y' + m_1 Y''' + [m_2 W Y' + m_3 W' Y] e^{(\alpha\mu(\zeta) - \frac{1}{2}\alpha^2\zeta)} = 0, \quad (12)$$

we have

$$\kappa W' + \beta Y Y' e^{\frac{-1}{2}\alpha^2 \zeta} E(e^\alpha \mu(\zeta)) = 0, \quad (13)$$

$$\kappa Y' + m_1 Y''' + [m_2 W Y' + m_3 W' Y] e^{\frac{-1}{2}\alpha^2 \zeta} E(e^\alpha \mu(\zeta)) = 0. \quad (14)$$

After using the Lemma in Eqs.(13-14), we have:

$$\kappa W' + \beta Y Y' = 0, \quad (15)$$

$$\kappa Y' + m_1 Y''' + m_2 W Y' + m_3 W' Y = 0. \quad (16)$$

On integrating the Eq. (15), we get:

$$W = \frac{-\beta}{2\kappa} Y^2 + C. \quad (17)$$

Plugging Eq. (17) in Eq. (16), we get:

$$m_1 Y''' - \left[\frac{\beta m_2}{2\kappa} + \frac{\beta m_3}{\kappa} \right] Y^2 Y' + [\kappa + C m_2] Y' = 0. \quad (18)$$

On integrating the Eq. (18), we get:

$$m_1 Y'' - \left[\frac{\beta m_2}{6\kappa} + \frac{\beta m_3}{3\kappa} \right] Y^3 + [\kappa + C m_2] Y = 0. \quad (19)$$

We suppose that the Eq. (5) has a form of solution as mention below:

$$Y(\xi) = \sum_{i=0}^n a_i U^i(\xi). \quad (20)$$

Where l_i and $i = 0, 1, 2, \dots, n$ are constant. By balancing principle as $n + 2 = 3n$, we get $n = 1$. Therefore, the initial solution becomes:

$$Y(\xi) = a_0 + a_1 U(\xi). \quad (21)$$

By substituting Eq. (21) into Eq. (17) and equating the coefficients of the distinct terms of U^i , a system of algebraic equations can be obtained as follows:

$$\begin{aligned}
(U)^0 &: Ca_0m_2 + \kappa a_0 + 2m_1 - \frac{\beta m_2 a_0^3}{2\kappa} - \frac{\beta m_3 a_0^3}{\kappa} = 0, \\
(U)^1 &: \kappa a_1 + Cm_2a_1 - 2m_1a_1 - \frac{3\beta m_2 a_0^2 a_1}{2\kappa} - \frac{3\beta m_3 a_0^2 a_1}{\kappa} = 0, \\
(U)^2 &: \kappa + Cm_2 - 8m_1 - \frac{3\beta m_2 a_0^2}{2\kappa} - \frac{3\beta m_2 a_0 a_1^2}{2\kappa} - \frac{3\beta m_3 a_0^2}{\kappa} - \frac{3\beta m_3 a_0 a_1^2}{\kappa} = 0, \\
(U)^3 &: 2m_1a_1 - \frac{\beta m_2 a_1^3}{\kappa} - \frac{\beta m_3 a_1^3}{\kappa} - \frac{3\beta m_2 a_0 a_1}{\kappa} - \frac{6\beta m_3 a_0 a_1}{\kappa} = 0, \\
(U)^4 &: 6m_1 - \frac{3\beta m_2 a_0^2}{2\kappa} - \frac{3\beta m_2 a_1^2}{2\kappa} - \frac{3\beta m_3 a_0}{\kappa} - \frac{3\beta m_3 a_1^2}{\kappa} = 0, \\
(U)^5 &: -\frac{3\beta m_2 a_1}{2\kappa} - \frac{3\beta m_3}{\kappa} = 0, \\
(U)^6 &: -\frac{\beta m_2}{2\kappa} - \frac{\beta m_3}{\kappa} = 0.
\end{aligned}$$

To solve the above equations with the support of Maple to get the successive solutions:

Set 1:

$$a_0 = 0, \quad a_1 = 2\sqrt{\frac{m_1\kappa}{\beta m_1 + 2\beta m_3}}, \quad \text{and} \quad C = -\frac{\kappa - 2m_1}{\beta_2}. \quad (22)$$

Set 2:

$$a_0 = 0, \quad a_1 = -2\sqrt{\frac{m_1\kappa}{\beta m_1 + 2\beta m_3}}, \quad \text{and} \quad C = -\frac{\kappa - 2m_1}{\beta_2}. \quad (23)$$

Inserting Eq. (23) and (22) into Eq. (21), we can determine the following solutions:

$$Y_1(\xi) = 2\sqrt{\frac{m_1\kappa}{\beta m_1 + 2\beta m_3}} \tanh(\xi). \quad (24)$$

$$Y_2(\xi) = -2\sqrt{\frac{m_1\kappa}{\beta m_1 + 2\beta m_3}} \tanh(\xi). \quad (25)$$

5 Physical Interpretation

In this section, the results presented in this work will be compared with those obtained by other scholars who utilized diverse methodologies. The governing equation has been the subject of exploration by various researchers, as outlined in the introduction section. The results presented in this study have been contrasted with the findings reported by Alsallami et al. (2023) and Al-Askar et al. (2022). In Al-Askar et al. (2022), authors employed the (G'/G) expansion method, yielding solutions in the form of exponential and trigonometric functions. Authors in Alsallami et al. (2023), on the other hand, employed Hirota's method to obtain solutions such as the cross-Kink rational and Homoclinic breather wave solutions. In comparison to these two papers, the present article introduces innovative outcomes in dynamic behavior. The results, involving hyperbolic functions tanh, extend beyond the

scope of the aforementioned papers. This distinction underscores the innovativeness of the findings presented in this article.

Furthermore, through the application of suitable parameter values, an array of varied formations such as dark solitons, V-shaped solitons, singular dark solitons, and bell-shaped solitons have been documented. To achieve this, we will utilize various parameter values that showcase distinct 2D and 3D graphs illustrating exclusive wave behaviors. By visualizing the arrangement and comprehending the related physical phenomena, we can observe a range of solutions represented by dark and bright shapes of solitons, along with bell-shaped solitons, periodic waves, kink solitons, and other types of solitons. The implementation of precise values for each parameter has allowed us to enhance numerous soliton features.

By selecting appropriate parameter values of Eq. (24), specifically $\beta = 0.2$, $m_1 = 0.02$, $m_2 = -0.5$, $m_3 = 0.03$, $\kappa = 0.7$, we obtain a predicted dark soliton as shown in Fig. 1. Dark solitons have garnered considerable attention in the field of non-linear optics due to their stable transmission properties. In optical fibers, a stable optical soliton typically emerges when there is a balance between Kerr nonlinearity and group velocity dispersion (GVD). Bright solitons propagate in regions characterized by anomalous dispersion, while dark solitons are transmitted in regions with normal dispersion. The distinguishing feature of solitons, whether dark or bright, is their particle-like nature during interactions. The 3D graph represents the interval $-7 < \eta < 7$ and $0 < \zeta < 7$. The 2D graph is plotted at different values of η as $\eta = 1, 5, 9$ within the range of $-4 < \zeta < 4$.

The solution of Eq. (24) exhibits a soliton with a V-shaped structure, characterized by different values of $m_1 = 0.002$ and $m_2 = 0.03$, as shown in Fig. 2. The 3D plot illustrates the range $0 < \eta < 4$ and $-4 < \zeta < 4$. The 2D plot demonstrates the variation of η at values of 1, 5, and 9 within the range $-4 < \zeta < 4$.

The solution of Eq. (24) yields a bell-shaped soliton with a minor change in the values of $m_1 = 1$ and the same value of $m_2 = 1$, as depicted in Fig. 3. The 3D plot illustrates the range $0 < \eta < 4$ and $-4 < \zeta < 4$. The 2D plot represents the variation of η at values of 0.1, 0.5, and 0.9 within the range $-4 < \zeta < 4$.

In Fig. 4, we illustrate the variation of time η with respect to ζ . We observe the impact of m_1 on fixed values of $m_2 = 1$. As the value of m_1 increases to 1.5, it exhibits discontinuity. The 3D plot represents the range $0 < \eta < 4$ and $-4 < \zeta < 4$. The 2D plot demonstrates the variation for η values of 0.1, 0.5, and 0.9 within the range $-4 < \zeta < 4$. In contrast to recent

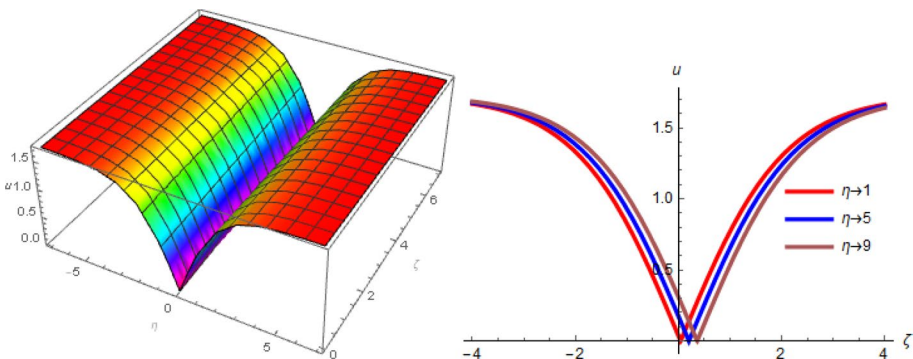


Fig. 1 3D and 2D graphs of Eq. (24)

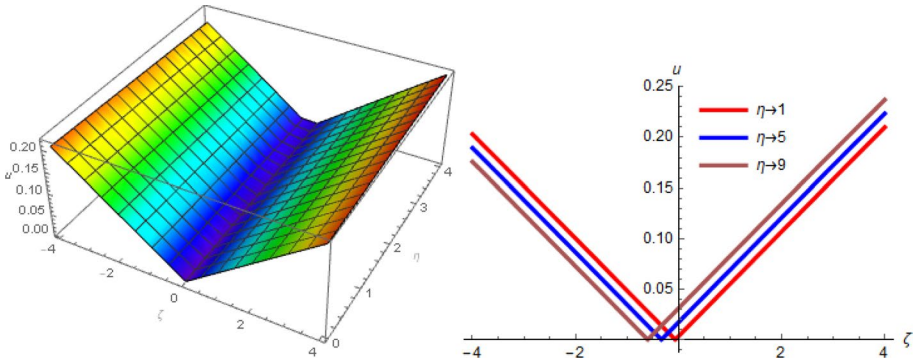


Fig. 2 3D and 2D graphs of Eq. (24)

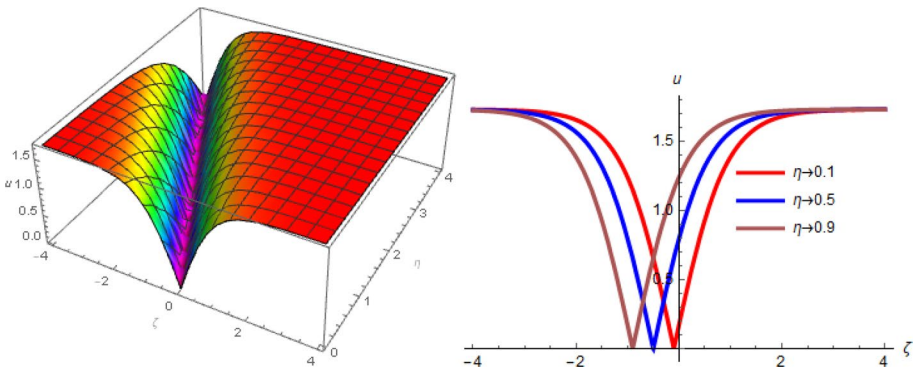


Fig. 3 3D and 2D graphs of Eq. (24)

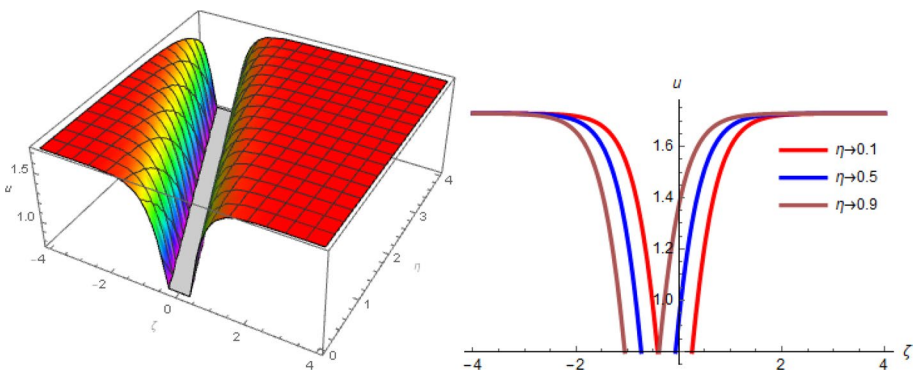


Fig. 4 3D and 2D graphs of Eq. (24)

literature, this paper presents novel solutions that have not been previously documented, as evidenced by a comparative analysis. These unique findings contribute innovatively to advancing our comprehension of soliton theory and the chaotic dynamics exhibited by

fractional-order nonlinear systems, thereby enhancing the overall understanding in this field. The significance of obtaining solutions for SFDSW equations lies in their importance and utility in understanding various essential physical phenomena across applied sciences, plasma physics, fluid mechanics and population dynamics.

6 Bifurcation theory

The concept of bifurcation refers to mathematical changes in the system and the quality of solutions provided by a group of differential equations. It is commonly used in the study of the mathematical structure of dynamic systems. Bifurcation occurs when a small change in the parameter values of a system leads to a sudden change in its behavior. It encompasses both local and global aspects of one-dimensional separation of operators operating in Banach's permanent spaces, demonstrating how the theory can be applied to problems involving split equality. Additionally, this concept delves into standard structures such as stability and the composition of the dividing solutions in detail.

Equation(1) is where the methodology of bifurcation analysis is applied. The Galilean translation Eq. (17) in a dynamic system, such as, is subjected to analysis study.

$$\begin{cases} \frac{dY}{dz} = P, \\ \frac{dP}{dz} = AY^3 - BY, \end{cases} \quad (26)$$

where $A = \frac{\beta m_2}{2m_1 \kappa} + \frac{\beta m_3}{m_1 \kappa}$ and $B = \frac{\kappa + Cm_2}{m_1}$. The above-mentioned system (26) contains two equilibrium points, which are given below:

$$Y_0 = (E_0, 0), Y_1 = (E_1, 0) \text{ and } Y_2 = (E_2, 0).$$

Here, the values of E_0 , E_1 , and E_2 are defined as follows:

$$E_0 = 0, E_1 = \sqrt{\frac{B}{A}}, \text{ and } E_2 = -\sqrt{\frac{B}{A}}.$$

In particular, we will introduce a specific type of bifurcation known as "Hopf bifurcation." This phenomenon occurs when a stable equilibrium point gives rise to periodic cycles as the bifurcation parameter reaches a critical value. This system will help us clarify the direction of classification for mathematical models. Homoclinic bifurcation, on the other hand, occurs when large invariant sets, such as periodic trajectories, intersect with the equilibrium point. This leads to a change in the topology of trajectories in phase space, which cannot be explained within a small region, unlike localized spatial bifurcation. In fact, the change in topology extends beyond what homoclinic bifurcation alone can account for.

Using the perspective of a dynamical system, the equilibrium points (P_i, Y_i) can be classified as follows: they are assigned as saddle points if $M^*(P_i, Y_i) < 0$, center points if $M^*(P_i, Y_i) > 0$ and the trace $\tau_1(P_i, Y_i) = 0$, nodes if $M^*(P_i, Y_i) > 0$ and $(\tau_1(P_i, Y_i))^2 - 4M^*(P_i, Y_i) > 0$, and zero points if $M^*(P_i, Y_i) = 0$ with a Hopf index of zero for (P_i, Y_i) . Here, M^* represents the Jacobian and τ_1 represents the trace of system (26).

- $A > 0, B < 0$

We have plotted the phase portrait for Fig. 5 using the given parameter values $A = 0.5$ and $B = -0.1$ for the equilibrium points $E_0 = (0, 0)$, $E_1 = (1, 0)$, and $E_2 = (-1, 0)$. At these points, there are two nonlinear periodic trajectories: $NPT(1, 0)$ at the equilibrium points $E_1 = (1, 0)$ and $E_2 = (-1, 0)$, and one super non-

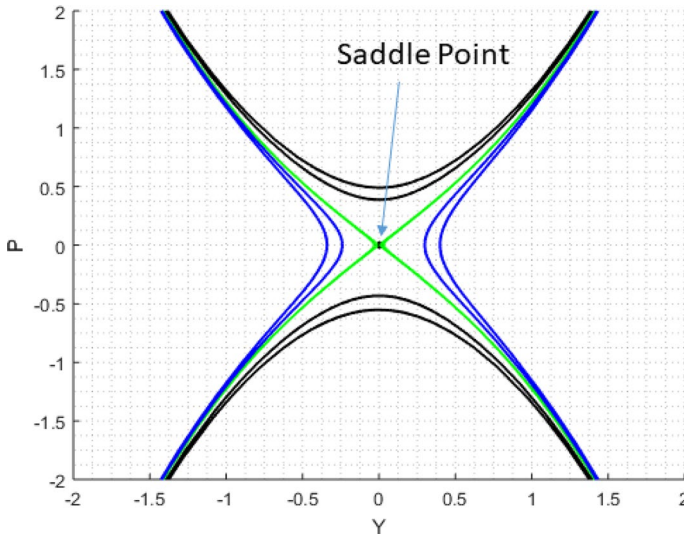


Fig. 5 Bifurcation phenomena of dynamical system (26)

linear periodic trajectory denoted as $SNPT(3, 1)$. Additionally, there is one non-linear homoclinic trajectory represented by $NHT(1, 0)$. Consequently, the equilibrium point $(0, 0)$ becomes a saddle point, while $E_1 = (1, 0)$ and $E_2 = (-1, 0)$ become center points, as shown in Fig. 5. Furthermore, the system (26) exhibits an infinite number of periodic trajectories both inside and outside the homoclinic trajectories, indicating the presence of an infinite number of periodic waves.

- $A > 0, B > 0$

In Fig. 6, we set $A = 0.6$ and $B = 0.3$. The system (26) has three equilibrium points, namely $E_0 = (0, 0)$, $E_1 = (1, 0)$, and $E_2 = (-1, 0)$ as shown in Fig. 6. There is only one nonlinear periodic trajectory $NPT(1, 0)$ and the center point is named as E_0 , while P is a saddle point for $NPT(1, 0)$. There are basically two saddle points, $E_1 = (1, 0)$ and $E_2 = (-1, 0)$. Therefore, the system has infinite periodic trajectories over $(0, 0)$ and open bounded trajectories on the right and left sides of E_1 and E_2 . Also, there are heteroclinic trajectories joining all the saddle points.

- $A < 0, B > 0$

In Fig. 7, we plotted the phase portrait for $A = -0.8, B = 0.5$. There is one non-linear periodic trajectory denoted as $NPT(1, 0)$ located at the center $E_0 = (0, 0)$. Thus, the system (26) has an infinite family of periodic trajectories over $(0, 0)$, which corresponds to an infinite periodic wave.

- $A < 0, B < 0$

In Fig. 8, we plotted the phase portrait for the given parameters $A = -0.5, B = -0.3$ as shown. There is one saddle point located at the center $E_0 = (0, 0)$ for open trajectories. Hence, the point $(0, 0)$ is the only equilibrium point. The saddle point implies that the system has an infinite number of open bounded trajectories.

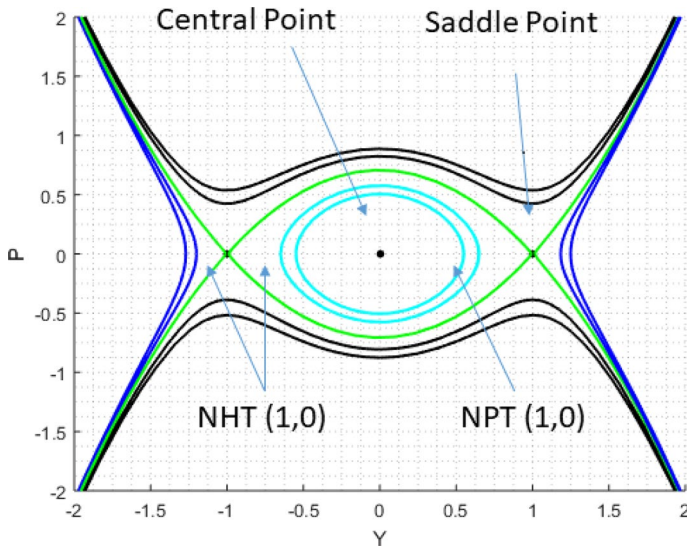


Fig. 6 Bifurcation phenomena of dynamical system(26)

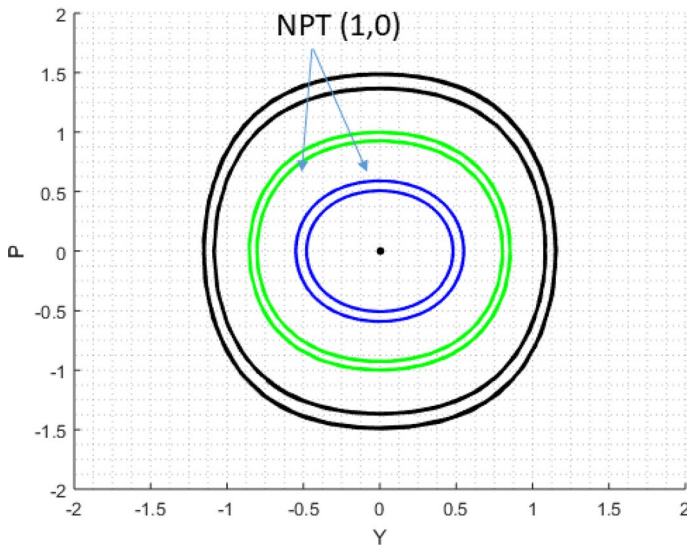


Fig. 7 Bifurcation phenomena of dynamical system(26)

7 Quasi-periodic and chaotic pattern

In mathematics, a quasiperiodic wave is a type of motion created by a dynamical system that contains a finite number of frequencies. To add more interest, the perturbed term $l_0 \cos(\omega t)$ is included in Eq. (1). Consequently, Eq. (10) with the perturbed term can be expressed as:

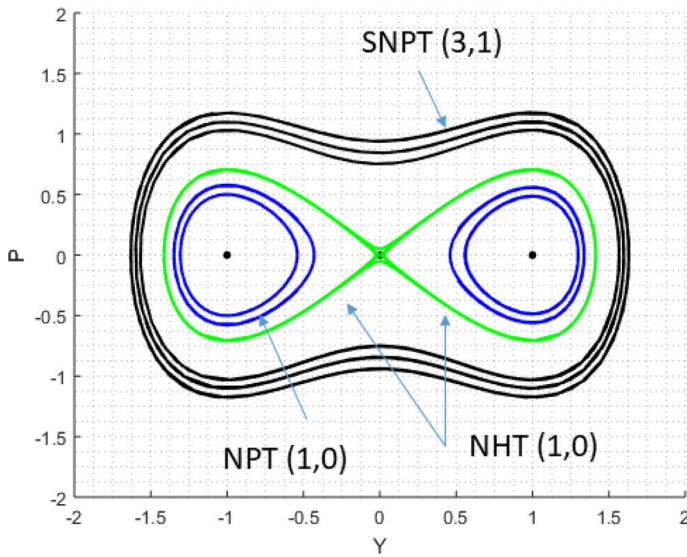


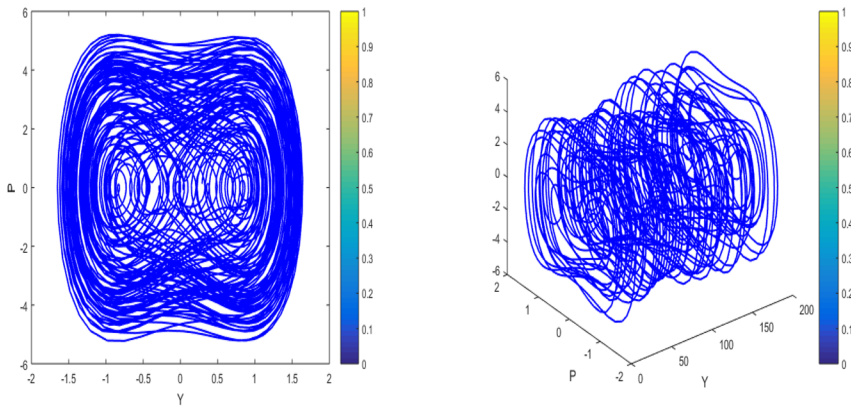
Fig. 8 Bifurcation phenomena of dynamical system (26)

$$\begin{cases} \frac{dY}{d\xi} = P, \\ \frac{dP}{d\xi} = AY^3 - BY + f_0 \cos(\omega t), \end{cases} \tag{27}$$

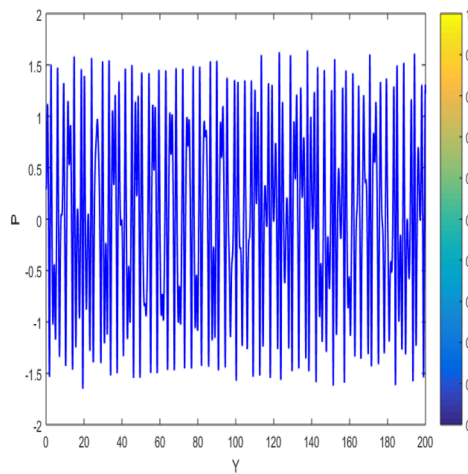
where ω is the frequency and f_0 represents the power of the perturbation. System (27) does not include the trivial force, i.e., it is not involved in Eq. (26). To investigate the periodic and quasiperiodic behavior of Eq. (1) with the existence of perturbation by unknown variables, we will examine the consequences of the frequency on the target model. Here, we will maintain visible limits of the considered system modifications and discuss the consequences of the power and frequency of the perturbation. Figure 9 shows a 3D phase portrait and a time series graph for $A = 0.6, B = 0.1,$ and $a = 0.5,$ with the initial conditions $(1.06, 1.1), f_0 = 1.05,$ and $\omega = 1.9.$ It is evident that a perturbed dynamical system (27) indicates periodic performance. While a specific pattern is found in three dimensions, outside of all these periodic waves, it can be seen in the time series graph, which continues to ensure periodic performance at particular values of the variables.

7.1 Case 1: $f_0 = 0$

By fixing $\omega = 1.1,$ the quasi-periodic behavior of the perturbed dynamical system (27) is shown in Fig. 9a–c. Figure 9a–c depict the time series, 2D phase portrait, and 3D phase portrait, respectively. The time series shows a steady curve, and the phase portrait exhibits a regular trajectory overlaid on the other. This observation demonstrates that the system is essentially quasi-periodic.



(a) phase portrait 2d, with perturbation term (b) phase portrait 3d, with perturbation term

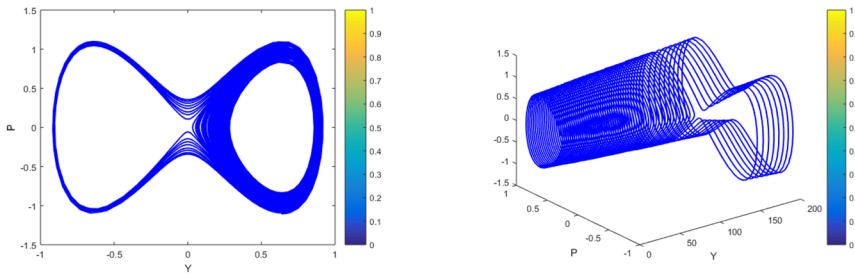


(c) Time series

Fig. 9 Quasi-periodic phenomena with perturbed dynamical system (27) for the initial values (0.29, 0.13) with $A = -13$, $B = 5.307$, $a = 0.1$, $f_0 = 4.5$ and $\omega = 2.1$

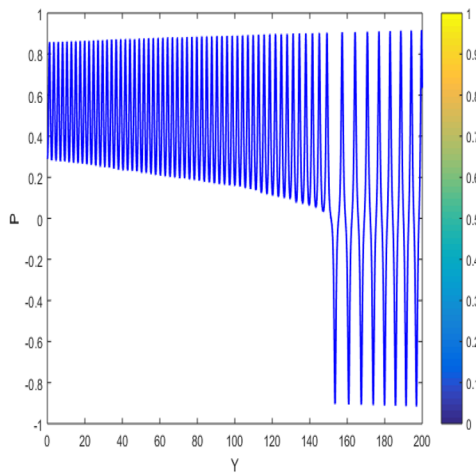
7.2 Case 2: $f_0 \neq 0$

We adjusted $f_0 = 1.05$ and used the same settings as in Fig. 9 to obtain Fig. 10a–c, which display the time series and phase portrait accordingly. The time series generates packets of identical amplitude across a defined time period, while the phase portrait exhibits a predictable trajectory overlaid on the other, albeit with a different shape than in Fig. 9. These graphs depict the quasi-periodicity of the system.



(a) phase portrait 2d, without perturbation term

(b) phase portrait 3d, without perturbation term



(c) Time series

Fig. 10 Quasi-periodic phenomena without perturbed dynamical system (27) for the initial values (0.29, 0.13) with $A = -13$, $B = 5.307$, $a = 0.1$, $f_0 = 0$ and $\omega = 2.1$

8 Sensitive analysis

We will now continue investigating periodic and quasi-periodic chaotic phenomena using the sensitivity behavior of a strong structural solution (27), with the following initial conditions: Navy blue color is used to indicate $(V, W) = (0.029, 0)$, while pink color is used to represent $(V, W) = (0.013, 0)$. In Fig. 11, two results are computed while maintaining similar parameters to Fig. 8. It is clear to observe that even small changes in initial values can disrupt the results, demonstrating the quasi-periodic chaotic behavior of the curve with these boundary values. In Fig. 12, using the initial condition $(V, W) = (0.75, 0)$ represented by Navy blue color and $(V, W) = (0.8, 0)$ with pink color, two solutions are reported with the same parameter measurements as shown in Fig. 7. It is noteworthy that even slight variations in the initial values have no effect on the results, further strengthening the claim for chaotic behavior. In Fig. 13, using the initial condition $(V, W) = (0.03, 0)$ represented by Navy blue color and $(V, W) = (0.01, 0)$ with pink color, the two results are shown by considering the same variable values as those taken in Fig. 5. It is known that minor changes

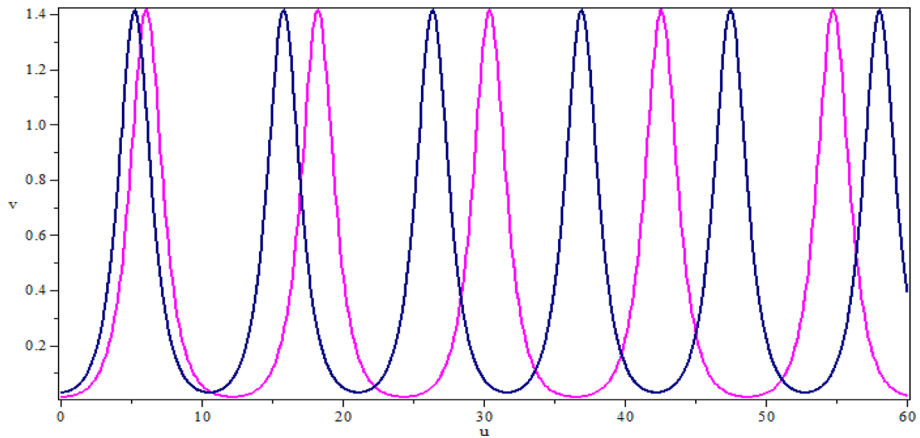


Fig. 11 Sensitivity behaviour of the dynamical system (26) with same parametric values taken in Fig. 8 with initial condition $(V, W) = (0.029, 0)$ in Navy blue color and $(V, W) = (0.013, 0)$ in pink color

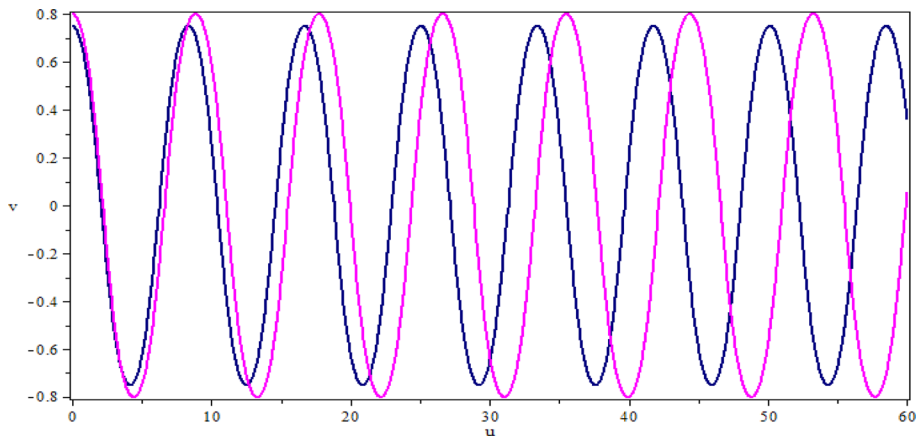


Fig. 12 Sensitivity behaviour of the dynamical system (26) with same parametric values taken in Fig. 7 with initial condition $(V, W) = (0.75, 0)$ in Navy blue color and $(V, W) = (0.8, 0)$ in pink color

in the initial conditions have an effect on the results of specific values, indicating the quasi-periodic chaotic nature of those values.

9 Multi-stability

This section will evaluate the multi-stability of the system (26). Multi-stability characterizes a flexible program with a limited parameter option, where diverse initial conditions result in the presence of two or more simultaneous outcomes. We employ a phase portrait and time series graphing approach to analyze the system (27) and explore its

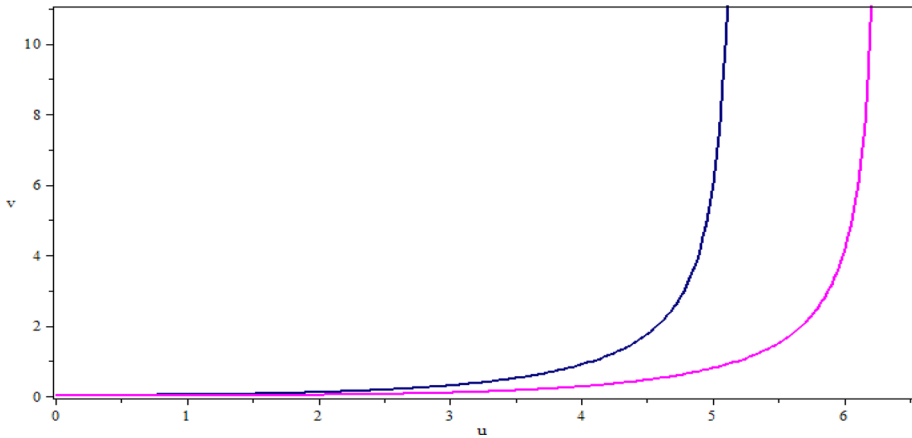


Fig. 13 Sensitivity behaviour of the dynamical system (26) with same parametric values taken in Fig. 5 with initial condition $(V, W) = (0.03, 0)$ in Navy blue color and $(V, W) = (0.01, 0)$ in pink color

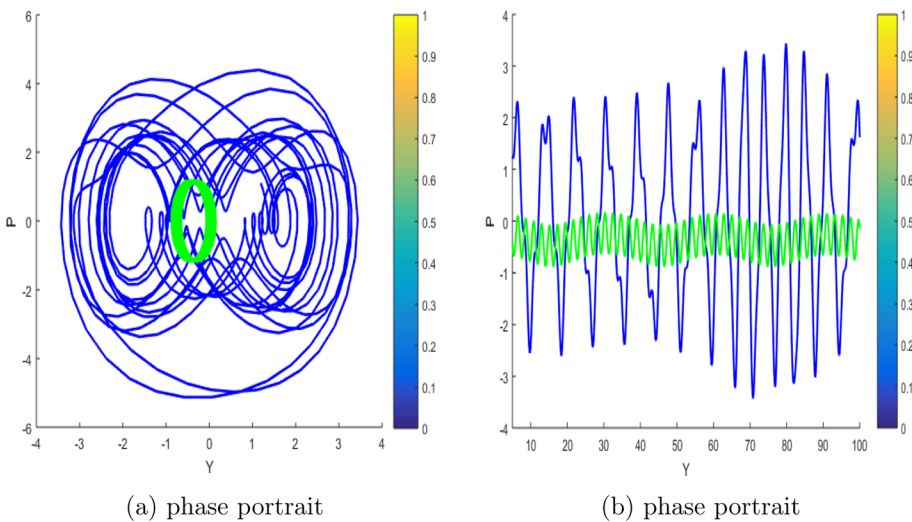


Fig. 14 Multi-stability of dynamical system (27) with fixed parametric values such as $a = 4.3$, $\omega = 2.9$, $A = 0.186$, $B = 0.07$ and $f_0 = 3.4067$ and different initial conditions $(V, W) = (1.19, 1.099)$ in blue colour and $(V, W) = (0.14, 0.099)$ in green colour

unique multi-stability characteristics. As shown in Fig. 14a, two separate snapshots are presented with parameter values $a = 4.3$, $\omega = 2.9$, $A = -0.186$, $B = 0.07$, and $f_0 = -3.4067$. The initial condition $(V, W) = (1.19, 1.099)$ is represented in blue, while the initial condition $(V, W) = (0.14, 0.099)$ is represented in green. When considering the initial condition $(V, W) = (1.19, 1.099)$, quasi-periodic behavior is observed, whereas the same set of primary variables $(V, W) = (0.14, 0.099)$ exhibits periodic behavior in the hypothetical system.

10 Conclusion

In this research, we effectively examined the stochastic-fractional Drinfel'd-Sokolov-Wilson model, a mathematical model applicable in the fields of electromagnetism and fluid mechanics. In our examination, we thoroughly scrutinized the equation through various lenses, encompassing soliton dynamics, bifurcation analysis, chaotic behaviors, and sensitivity analysis. Initially, we employed the tanh technique to identify the traveling wave solutions of the model, enabling the establishment of soliton solutions depicted in Figs. 1, 2, 3 and 4. Various categories of soliton solutions, including dark solitons, bell-shape solitons, and more, were observed in the models. The updated discussion revealed that the reported soliton solutions are novel and have not been previously documented in the literature. Additionally, we observed bifurcation, the qualitative behavior of quasi-periodic nonlinear waves and chaotic behaviors within the dynamical system, illustrating corresponding phase portraits as shown in Figs. 5, 6, 7, 8, 9 and 10. It was evident that the observed model exhibits waves of nonlinear and super nonlinear periodicity. Lastly, an investigation has been conducted into the system's sensitivity and multistability to initial conditions as presented in Figs. 11, 12, 13 and 14. It is anticipated that the results presented in this study, such as bifurcation, periodic and quasi-periodic behavior, chaos, sensitivity, and multi-stability, have implications for a wide range of nonlinear phenomena in the world. In contrast to recent literature, this paper presents novel solutions, as evidenced by a comparative analysis. The results, previously unreported, contribute innovatively to the comprehension of soliton theory and the chaotic tendencies within fractional order nonlinear systems. These groundbreaking findings not only advance our understanding but also lay the groundwork for refining research methodologies. Moving forward, this work serves as a catalyst for continued exploration into the dynamics of nonlinear systems. Therefore, this study may inspire further research into various nonlinear challenges.

Acknowledgements The researchers would like to acknowledge Deanship of Scientific Research, Taif University for funding this work.

This project has been partially supported by Gulf University for Science and Technology and the Centre for Applied Mathematics and Bio-informatics (CAMB) under project code: ISG-3.

Author Contributions ARA and AJ Conceptualization, writing original draft, software; MI and MBR validation, investigation, resources; AJ supervision, formal analysis, review and editing. All authors equally contributed and approved for submission.

Funding Open access funding provided by the Scientific and Technological Research Council of Türkiye (TÜBİTAK). Not available

Data availability All generated and analysed results which have obtained during this research are included in the manuscript.

Data sharing not applicable to this article as no data sets were generated or analysed during the current study.

Declarations

Conflict of interest The authors declare that they have no conflict of interest.

Ethical approval Not applicable.

Consent for publication Not applicable.

Open Access This article is licensed under a Creative Commons Attribution 4.0 International License, which permits use, sharing, adaptation, distribution and reproduction in any medium or format, as long as you give appropriate credit to the original author(s) and the source, provide a link to the Creative Commons licence, and indicate if changes were made. The images or other third party material in this article are included in the article's Creative Commons licence, unless indicated otherwise in a credit line to the material. If material is not included in the article's Creative Commons licence and your intended use is not permitted by statutory regulation or exceeds the permitted use, you will need to obtain permission directly from the copyright holder. To view a copy of this licence, visit <http://creativecommons.org/licenses/by/4.0/>.

References

- Ablowitz, M.J., Kaup, D.J., Newell, A.C., Segur, H.: The inverse scattering transform-Fourier analysis for nonlinear problems. *Stud. Appl. Math.* **53**(4), 249–315 (1974)
- Ahmed, N., Mannan, A., Chowdhury, N.A., Mamun, A.A.: Electrostatic rogue waves in double pair plasmas, chaos: an interdisciplinary. *J. Nonlin. Sci.* **28**(12), 123107 (2018)
- Akbar, M.A., Akinyemi, L., Yao, S.W., Jhangeer, A., Rezazadeh, H., Khater, M.M.A., Ahmad, H., Inc, M.: Soliton solutions to the Boussinesq equation through sine-Gordon method and Kudryashov method. *Results Phys.* **25**, 104228 (2021)
- Akbar, M.A., Wazwaz, A.M., Mahmud, F., Baleanu, D., Roy, R., Barman, H.K., Mahmoud, W., Al Sharif, M.A., Osman, M.S.: Dynamical behavior of solitons of the perturbed nonlinear Schrödinger equation and microtubules through the generalized Kudryashov scheme. *Results Phys.* **43**, 106079 (2022)
- Akbar, M.A., Abdullah, F.A., Islam, M.T., Al Sharif, M.A., Osman, M.S.: New solutions of the soliton type of shallow water waves and superconductivity models. *Results Phys.* **44**, 106180 (2023)
- Akinyemi, L., Rezazadeh, H., Shi, Q.H., Inc, M., Khater, M.M.A., Ahmad, H., Jhangeer, A., Akbar, M.A.: New optical solitons of perturbed nonlinear Schrödinger-Hirota equation with spatio-temporal dispersion. *Results Phys.* **29**, 104656 (2021)
- Al-Askar, F.M., Cesarano, C., Mohammed, W.W.: The Analytical Solutions of Stochastic-Fractional Drinfel'd-Sokolov-Wilson, Equations via $\frac{G'}{G}$ -Expansion Method. *Symmetry* **14**(10), 2105 (2022)
- Al-Askar, F.M., Cesarano, C., Mohammed, W.W.: The analytical solutions of stochastic-fractional Drinfel'd-Sokolov-Wilson equations via (G'/G) -expansion method. *Symmetry* **14**(10), 2105 (2022)
- Al-Askar, F.M., Mohammed, W.W., Samura, S.K., El-Morshedy, M.: The exact solutions for fractional-stochastic Drinfel'd-Sokolov-Wilson equations using a conformable operator. *J. Funct. Spaces* (2022). <https://doi.org/10.1155/2022/7133824>
- Almusawa, H., Jhangeer, A., Hussain, Z.: Observation on different dynamics of breaking soliton equation by bifurcation analysis and multistability theory. *Results Phys.* **36**, 105364 (2022)
- Alsallami, S.A., Rizvi, S.T., Seadawy, A.R.: Study of Stochastic-Fractional Drinfel'd-Sokolov-Wilson equation for M-shaped rational, homoclinic breather, periodic and kink-cross rational solutions. *Mathematics* **11**(6), 1504 (2023)
- Anderson, D.R., Ulness, D.J.: Properties of the Katugampola fractional derivative with potential application in quantum mechanics. *J. Math. Phys.* **56**(6), 063502 (2015)
- Arefin, M.A., Khatun, M.A., Uddin, M.H., İnç, M.: Investigation of adequate closed form travelling wave solution to the space-time fractional non-linear evolution equations. *J. Ocean Eng. Sci.* **7**(3), 292–303 (2022)
- Bains, A.S., Misra, A.P., Saini, N.S., Gill, T.S.: Modulational instability of ion-acoustic wave envelopes in magnetized quantum electron-positron-ion plasmas. *Phys. Plasmas* **17**(1), 012103 (2010)
- Baluku, T.K., Hellberg, M.A.: Dust acoustic solitons in plasmas with kappa-distributed electrons and/or ions. *Phys. Plasmas* **15**(12), 123705 (2008)
- Bo, W.B., Wang, R.R., Fang, Y., Wang, Y.Y., Dai, C.Q.: Prediction and dynamical evolution of multipole soliton families in fractional Schrödinger equation with the PT-symmetric potential and saturable nonlinearity. *Nonlinear Dyn.* **111**(2), 1577–1588 (2023)
- Calin, O.: An informal introduction to stochastic calculus with applications (2015)
- Drinfeld, V.G., Sokolov, V.V.: Equations of Korteweg-de Vries type, and simple Lie algebras, In *Doklady Akademii Nauk*, (Vol. 258, No. 1, pp. 11–16), Russian Academy of Sciences (1981)
- El-Taibany, W.F., Sabry, R.: Dust-acoustic solitary waves and double layers in a magnetized dusty plasma with nonthermal ions and dust charge variation. *Phys. Plasmas* **12**, 082302 (2005)
- Geng, K.L., Zhu, B.W., Cao, Q.H., Dai, C.Q., Wang, Y.Y.: Nondegenerate soliton dynamics of nonlocal nonlinear Schrödinger equation. *Nonlinear Dyn.* **111**(17), 16483–16496 (2023)

- Geng, K.L., Mou, D.S., Dai, C.Q.: Nondegenerate solitons of 2-coupled mixed derivative nonlinear Schrödinger equations. *Nonlinear Dyn.* **111**(1), 603–617 (2023)
- Ghosh, U.N., Chatterjee, P., Roychoudhury, R.: The effect of q-distributed electrons on the head-on collision of ion-acoustic solitary waves. *Phys. Plasmas* **19**(1), 012113 (2012)
- Gupta, A., Ganesh, R., Joy, A.: Kolmogorov flow in two dimensional strongly coupled Yukawa liquid: a molecular dynamics study. *Phys. Plasmas* **22**(10), 103706 (2015)
- Hirota, R.: The direct method in soliton theory, p. 155. Cambridge University Press, Cambridge (2004)
- Hoffman, J.D., Frankel, S.: Numerical methods for engineers and scientists. CRC Press, Cambridge (2018)
- Imkeller, P., Monahan, A.H.: Conceptual stochastic climate models. *World Scientific* **2**, 311–326 (2002)
- Islam, M.T., Akter, M.A., Ryehan, S., Gómez-Aguilar, J.F., Akbar, M.A.: A variety of solitons on the oceans exposed by the Kadomtsev Petviashvili-modified equal width equation adopting different techniques. *J. Ocean Eng. Sci.* (2022). <https://doi.org/10.1016/j.joes.2022.07.001>
- Islam, M.T., Akbar, M.A., Gómez-Aguilar, J.F., Bonyah, E., Fernandez-Anaya, G.: Assorted soliton structures of solutions for fractional nonlinear Schrodinger types evolution equations. *J. Ocean Eng. Sci.* **7**(6), 528–535 (2022)
- Islam, M.T., Ryehan, S., Abdullah, F.A., Gomez-Aguilar, J.F.: The effect of Brownian motion and noise strength on solutions of stochastic Bogoyavlenskii model alongside conformable fractional derivative. *Optik* **287**, 171140 (2023)
- Jahan, S., Chowdhury, N.A., Mannan, A., Mamun, A.A.: Modulated dust-acoustic wave packets in an opposite polarity dusty plasma system. *Commun. Theor. Phys.* **71**(3), 327–333 (2019)
- Jansen, H., Boer, M.D., Unnikrishnan, S., Louwerse, M., Elwenspoek, M.: Black silicon method X: a review on high speed and selective plasma etching of silicon with profile control: an in-depth comparison between Bosch and cryostat DRIE processes as a roadmap to next-generation equipment. *J. Micro-mech. Microeng.* **19**(3), 033001 (2009)
- Khatun, M.A., Arefin, M.A., Islam, M.Z., Akbar, M.A., Uddin, M.H.: New dynamical soliton propagation of fractional type couple modified equal-width and Boussinesq equations. *Alex. Eng. J.* **61**(12), 9949–9963 (2022)
- Liu, H., Yang, H., Liu, N., Yang, L.: Bifurcation and chaos analysis of tumor growth. *Int. J. Biomath.* **15**(6), 2250039 (2022)
- Matveev, V.B., Salle, M.A.: *Darboux transformations and solitons*, p. 17. Springer, Berlin and Heidelberg (1991)
- Prévôt, C., Röckner, M.: A concise course on stochastic partial differential equations, pp. 105–148. Springer, Berlin (2007)
- Ren, B., Lou, Z.M., Liang, Z.F., Tang, X.Y.: Nonlocal symmetry and explicit solutions for Drinfeld-Sokolov-Wilson system. *Eur. Phys. J. Plus* **131**, 1–9 (2016)
- Saha, A.: Bifurcation, periodic and chaotic motions of the modified equal width-Burgers (MEW-Burgers) equation with external periodic perturbation. *Nonlinear Dyn.* **87**(4), 2193–201 (2017)
- Sahoo, S., Ray, S.S.: New double-periodic solutions of fractional Drinfeld-Sokolov-Wilson equation in shallow water waves. *Nonlin. Dyn.* **88**, 1869–1882 (2017)
- Samina, S., Jhangeer, A., Chen, Z.: Bifurcation, chaotic and multistability analysis of the (2+1)-dimensional elliptic nonlinear Schrödinger equation with external perturbation. *Waves Random Complex Media* (2022). <https://doi.org/10.1080/17455030.2022.2121010>
- Sokolov, V.V.: Lie algebras and equations of Korteweg-de Vries type. *Curr. Probl. Math.* **24**, 81–180 (1984)
- Sprott, J.C.: A proposed standard for the publication of new chaotic systems. *Int. J. Bifur. Chaos* **21**(09), 2391–2394 (2011)
- Talafha, A.M., Jhangeer, A., Kazmi, S.S.: Dynamical analysis of (4+ 1)-dimensional Davey Stewartson Kadomtsev Petviashvili equation by employing Lie symmetry approach. *Ain Shams Eng. J.* **14**(11), 102537 (2023)
- Vivas-Cortez, M., Raza, N., Kazmi, S.S., Chahlaoui, Y., Basendwah, G.A.: A novel investigation of dynamical behavior to describe nonlinear wave motion in (3+ 1)-dimensions. *Results Phys* **55**, 107131 (2023)
- Wang, K.J., Wang, G.D.: He's variational method for the time-space fractional nonlinear Drinfeld-Sokolov-Wilson system. *Math. Meth. Appl. Sci.* **46**(7), 7798–7806 (2023)
- Wang, R.R., Wang, Y.Y., Dai, C.Q.: Influence of higher-order nonlinear effects on optical solitons of the complex Swift-Hohenberg model in the mode-locked fiber laser. *Opt. Laser Technol.* **152**, 108103 (2022)
- Wen, X.K., Jiang, J.H., Liu, W., Dai, C.Q.: Abundant vector soliton prediction and model parameter discovery of the coupled mixed derivative nonlinear Schrödinger equation, *Nonlinear Dynamics*, pp. 1–13 (2023)
- Wilson, G.: The affine Lie algebra $C(1) 2$ and an equation of Hirota and Satsuma. *Phys. Lett. A* **89**(7), 332–334 (1982)

- Xu, S.Y., Zhou, Q., Liu, W.: Prediction of soliton evolution and equation parameters for NLS-MB equation based on the phPINN algorithm. *Nonlinear Dyn.* **111**(19), 18401–18417 (2023)
- Yang, X., Wang, C.L., Liu, C.B., Zhang, J.R., Shi, Y.R., Jian-Rong, W.S., Duan, L. Yang.: The collision effect between dust grains and ions to the dust ion-acoustic waves in a dusty plasma. *Phys. Plasmas* **19**(10), 103705 (2012)
- Yokuş, A., Durur, H., Duran, S., Islam, M.T.: Ample felicitous wave structures for fractional foam drainage equation modeling for fluid-flow mechanism. *Comput. Appl. Math.* **41**(4), 174 (2022)
- Zaman, U.H.M., Arefin, M.A., Akbar, M.A., Uddin, M.H.: Study of the soliton propagation of the fractional nonlinear type evolution equation through a novel technique. *PLoS ONE* **18**(5), e0285178 (2023)
- Zaman, U.H.M., Arefin, M.A., Akbar, M.A., Uddin, M.H.: Stable and effective traveling wave solutions to the non-linear fractional Gardner and Zakharov-Kuznetsov-Benjamin-Bona-Mahony equations. *Partial Diff. Equ. Appl. Math.* **7**, 100509 (2023)
- Zaman, U.H.M., Arefin, M.A., Akbar, M.A., Uddin, M.H.: Utilizing the extended tanh-function technique to scrutinize fractional order nonlinear partial differential equations. *Part. Diff. Equ. Appl. Math.* **8**, 100563 (2023)
- Zhang, K., Han, T.: The optical soliton solutions of nonlinear Schrödinger equation with quintic non-Kerr nonlinear term. *Results Phys.* **48**, 106397 (2023)

Publisher's Note Springer Nature remains neutral with regard to jurisdictional claims in published maps and institutional affiliations.

Authors and Affiliations

Ali R. Ansari¹ · Adil Jhangeer^{2,6} · Mudassar Imran³ · A. S. A. Alsubaie⁴ · Mustafa Inc⁵

✉ Mustafa Inc
minc@firat.edu.tr

Ali R. Ansari
ansari.a@gust.edu.kw

Adil Jhangeer
adil.jhangeer@gmail.com

Mudassar Imran
mudassar.imran@ajman.ac.ae

A. S. A. Alsubaie
asubaie@tu.edu.sa

- ¹ Centre for Applied Mathematics and Bioinformatics (CAMB), Gulf University for Science and Technology, West Mishref, Kuwait
- ² Department of Mathematics, Namal University, 30 KM Talagang Road, Mianwali 42250, Pakistan
- ³ College of Humanities and Sciences, Ajman University, Ajman, United Arab Emirates
- ⁴ Department of Physics, College of Khurma University College, Taif University, P.O. Box 11099, 21944 Taif, Saudi Arabia
- ⁵ Department of Mathematics, Firat University, 23119 Elazig, Turkey
- ⁶ VSB – Technical University of Ostrava, Ostrava-Poruba, Czech Republic